Optimization and phase transitions in a chaotic model of data traffic

M. Woolf,[1,2] D. K. Arrowsmith,[1] R. J. Mondragón-C,[2] and J. M. Pitts[2]
[1]*Mathematics Research Centre, Queen Mary, University of London, London E1 4NS, United Kingdom*
[2]*Department of Electronic Engineering, Queen Mary, University of London, London E1 4NS, United Kingdom*
(Received 30 January 2002; revised manuscript received 3 May 2002; published 10 October 2002)

Ohira and Sawatari [Phys. Rev E **58**, 193 (1998)] introduced a simple model for a packet-switching network which was extended by Solé and Valverde [Physica A **289**, 595 (2001)]. Both models used Poisson-like traffic sources. Solé and Valverde demonstrated that long-range dependence (LRD) in autocorrelation behavior can be seen in the queue length dynamics at a given node. Actual network traffic sources are known to exhibit long-range autocorrelation. To simulate the real case more closely, we have studied the effect of introducing LRD behavior at an earlier stage. We replaced the Poisson-like sources with LRD sources, modeled using chaotic maps. As was seen in the previous models, a phase transition occurs as the traffic load on a network is increased and the network changes to a congested state where the time taken for delivery of packets increases dramatically and throughput collapses. The paper reports extensive numerical results from our simulations using both Poisson and LRD sources. It demonstrates the natural network-induced LRD when sources are purely Poisson and shows strong enhancement when LRD sources are added. The model is adapted to include congestion control mechanisms and their impact is considered.

DOI: 10.1103/PhysRevE.66.046106 PACS number(s): 89.40.+k, 05.45.−a

I. INTRODUCTION

Extensive measurements of real network traffic have shown that the autocorrelation of the packet rates decays as a power law [1,2]. This behavior is said to be *self-similar* and to display *long-range dependence* (LRD) [3]. This phenomenon results in increased queue lengths and delays, and cannot be ''washed out'' by mixing sources of data. The effects of LRD need to be allowed for, both in computer models of network behavior and in the routing algorithms used to control data flow through networks. In this paper we look at a previously developed model of a network, Ref. [4], that was used to illustrate the emergence of congestion in a network. LRD was observed in this model, but this arose from interaction within the network and was not intrinsic to the traffic sources, or *hosts*, which are Poisson-like. We compare Poisson sources with LRD sources at the same load values. Both the LRD sources and Poisson sources are modeled using chaotic maps. Thus we are able to introduce LRD directly at the host level, which allows a study of the ''hierarchical'' nature of LRD from various sources, and models the real situation more closely. The implementation of control of host queue lengths also brings new insights into the model's behavior.

The paper is organized as follows. The history and features of the network model are described. The main aspect of the paper is the introduction of chaotic maps for the production of packet traffic sources within the network. The sources can be continuously varied to give traffic across the full range of the Hurst parameter $H \in (\frac{1}{2},1)$. Mean field models are introduced for the network in steady state, that enable the calculation of a critical point for the load on the network at which the average lifetime of a packet changes dramatically. The two models are distinguished in that global and local conditions are used for the congestion criticality condition. Their accuracy relative to other experimental results is shown.

Comparisons are made of the phase transition using experiments with the two types of source. Simulations with LRD sources show average packet lifetimes to be much higher before the phase transition and throughput somewhat lower at the transition. Measuring time series of average queue lengths showed that LRD sources greatly change the way that queues build up in the network even at very small traffic loads. The effect that the different sources had on the LRD character of packet delay times seen in the original model is investigated and how this changed with both the load and the distance packets had traveled. Further experimental behavior is processed using ''R/S'' statistics (defined later and referenced here) [3,5], which again confirms a critical value of the load in agreement with the other indicators. Finally, we extend the scope of the original to accommodate control strategies on the lengths of host queues and examine the changed throughput behavior.

II. MODEL OF NETWORKED DATA TRAFFIC

Our model for network traffic is similar to those described in Refs. [4,6,7] and to the cellular automaton model of Ref. [8]. The network architecture is a square lattice in which each node has four neighbors. As in Fig. 1 of Solé and Valverde [4], there are two types of nodes. Routers only store and forward packets; hosts can also generate packets. The density of hosts $\rho \in [0,1]$ is the ratio between the number of hosts and the total number of nodes in the network. Hosts are randomly distributed throughout the network. The finite rectangular lattice $\mathcal{Z}$ consists of L^2 nodes. The position of the each node in the lattice $\mathcal{Z}$ is given by the coordinate vector $\mathbf{r}=(i,j)$, where i and j are integers in the range 1 to L.

We use periodic boundary conditions throughout. Hence the network can be seen as having a toroidal topology in which nodes on one edge of the lattice are connected to nodes on the opposite edge. To measure the distance between a pair of nodes the periodic Manhattan metric

$$d_{\mathrm{PM}}(\mathbf{r}_1,\mathbf{r}_2)=L-\left|\left|i_2-i_1\right|-\frac{L}{2}\right|-\left|\left|j_2-j_1\right|-\frac{L}{2}\right| \qquad (1)$$

is used, where the points $\mathbf{r}_1=(i_1,j_1)$ and $\mathbf{r}_2=(i_2,j_2)$ of $\mathcal{Z}$ give the positions of the two nodes. Each node has a queue of unlimited length in which to store packets.

Previous simulations of packet traffic generation at each host have used Poisson (or Markovian) distributions. In this case a packet is generated at a host only if a random number on the $[0,1]$ interval is below a discriminator value λ. Hence, for a uniform random distribution the average rate at which packets are produced at a host is λ.

An alternative to this is to use chaotic maps to model the LRD nature of real packet traffic. We used the family of maps $f=f_{(m_1,m_2,d)}:I\to I$ defined on the unit interval I by $x_{n+1}=f(x_n)$ where

$$x_{n+1}=\begin{cases} x_n+(1-d)\left(\dfrac{x_n}{d}\right)^{m_1}, & x_n\in[0,d] \\ x_n-d\left(\dfrac{1-x_n}{1-d}\right)^{m_2}, & x_n\in(d,1], \end{cases} \qquad (2)$$

described in previous papers (see Erramilli *et al.* [9]), and related maps in Refs. [10,11]. Here $d\in(0,1)$ and the parameters $m_1,m_2\in(\frac{3}{2},2)$ induce *intermittency* at each of the points $x=0$ and $x=1$. The orbital ''escape times'' in neighborhoods of 0 and 1 become power-law dependent. If this map is iterated a large number of times, the values of x_n will form a nonuniform continuous distribution on the interval I. The parameter d is used as a discriminator, as λ is for the Poisson case. If x_n falls between 0 and d, a packet is generated; and if x_n falls between d and 1, no packet is generated. Thus we have a discrete output map associated with the function (3), which is

$$y(x_n)=\begin{cases} 1, & x_n\in[0,d] \\ 0, & x_n\in(d,1]. \end{cases} \qquad (3)$$

The intermittency behavior of the map f induces the so-called ''memory'' in the digital output y_n giving the long-range correlation effects required for the packet traffic. This feature is shown by the slow decay of variance with respect to n, the size of batched output, see Fig. 1(b) and Ref. [1]. An example of this phenomenon is illustrated in Fig. 1(a) where a sequence of the iterated values x near the origin have small increments. This effect is even stronger for orbits passing closer to $x=0$. The time of escape (i.e., into the region $x>d$) of an orbit from a neighborhood of the origin has a power-law dependence on its initial position [10].

The nonlinear nature of f means that in this case the load $\lambda=\lambda(m_1,m_2,d)$ (i.e., the average value of the output y per iteration) is not equal to d, but is given by $\lambda=\int_0^d\mu(x)dx$, where μ is the natural invariant density distribution of the map f on the interval $[0,d]$. This distribution has no closed form and is often obtained numerically via the Perron-Frobenius operator [12]. Thus the various statistical properties of traffic generated in this way are determined by the map's parameters m_1, m_2, and d. For example, the autocorrelation vector $c(n)$, $n\in\mathbb{Z}^+$, of the output function y is known to have asymptotic behavior $c(n)\sim n^{-\beta}$, up to a multiplicative constant, as $n\to\infty$ with $\beta=(2-m)/(m-1)\in(0,1)$ for $m=\max\{m_1,m_2\}$ with $m_1,m_2\in(\frac{3}{2},2)$. Furthermore, the Hurst parameter, H, is given by

$$H=1-\frac{\beta}{2}=\frac{3m-4}{2m-2} \qquad (4)$$

and ranges over the interval $(\frac{1}{2},1)$, [13–15]. Thus $m_1,m_2=1.5$ corresponds to Poisson-like behavior and as m_1,m_2 are increased towards 2, the behavior is increasingly long-range dependent, see Refs. [13,15].

A routing algorithm is needed to model the dynamic aspects of the network. Packets are created at hosts and sent through the lattice one step at a time until they reach their destination host. In real packet-switching networks, packets carry header and information payloads, including data about the state of the network with them. To simplify the modeling, we only record the time of creation and the source and destination addresses when passing packets through the network.

The routing algorithm operates as follows

(1) First a host creates a packet following either a uniform random distribution (Poisson) or a distribution defined by a chaotic map (LRD), as described above. If a packet is generated it is put at the end of the queue for that host. This is repeated for each host in the lattice.

(2) Packets at the head of each queue are picked up and sent to a neighboring node selected according to the following rules. (a) A neighbor closest to the destination node is selected. (b) If more than one neighbor is at the minimum distance from the destination, the link through which the smallest number of packets have been forwarded is selected. (c) If more than one of these links shares the same minimum number of packets forwarded, then a random selection is made.

This process is repeated for each node in the lattice. The whole procedure of packet generation and movement represents one time step of the simulation. Initially, there is no feedback implemented on queue lengths in this algorithm and hence the model is uncontrolled. This is a scenario similar to the one discussed by Solé and Valverde in Ref. [4]. In Fig. 2(a) we have clear evidence of the earlier onset of congestion in the LRD traffic by comparison with the Poisson traffic produced at the same rate when this routing algorithm is implemented. Although the throughput is only slightly reduced, the average lifetimes increase by up to a factor of 10. This earlier onset appears to be the most important feature of LRD congestion within the context of the model, and has significant implications for shared backbone data network infrastructures.

III. MODELS FOR SUBCRITICAL NETWORK BEHAVIOR

Here we develop two simple mean field models to estimate local and global load conditions at the boundary of

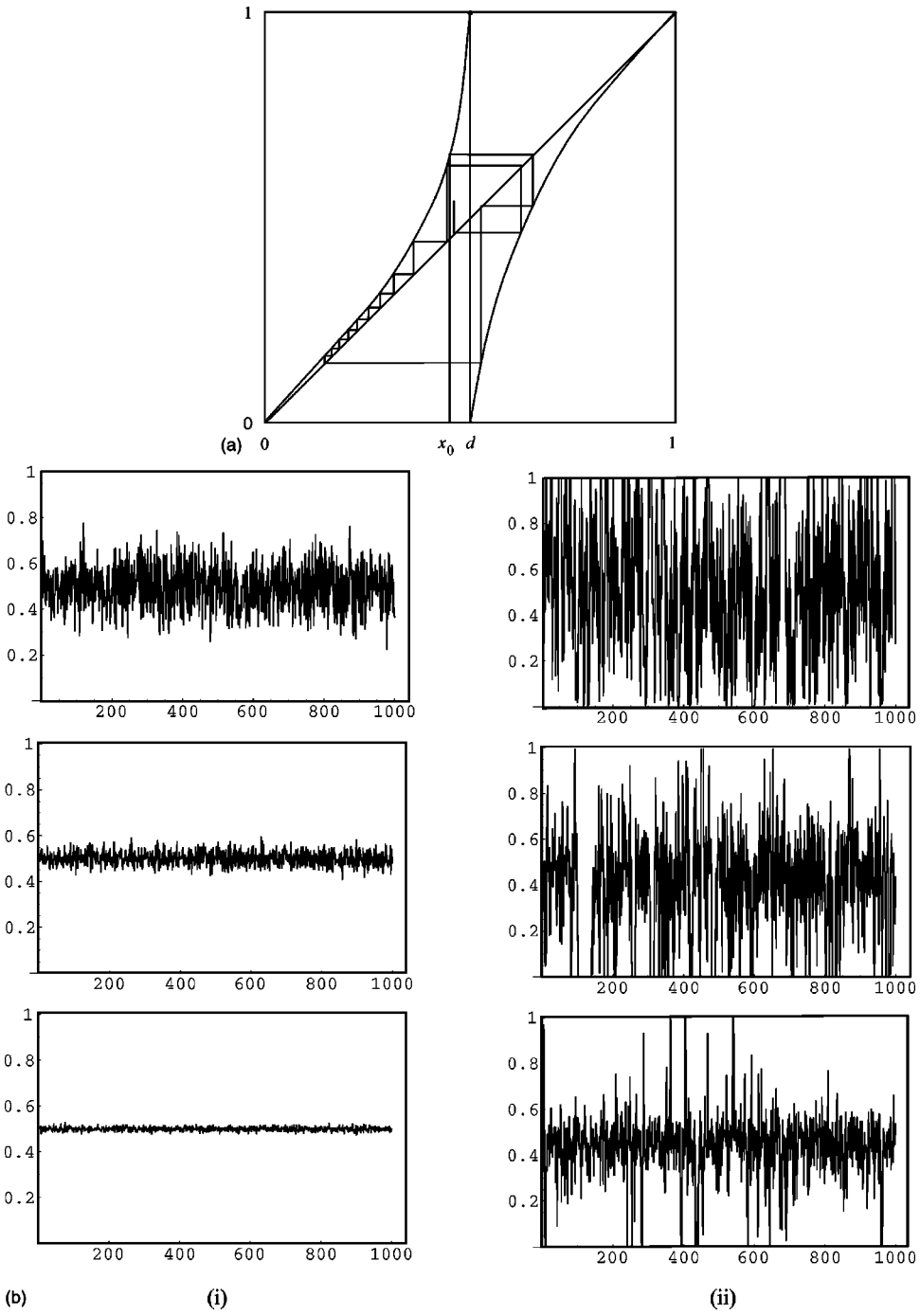

FIG. 1. (a) The piecewise continuous graph of a map f described by Eq. (2) with $f(x)$ plotted against x. An intermittent orbit of f is illustrated with initial condition x_0. (b) Averaged binary output from (i) a Poisson-like source and (ii) a chaotic intermittent source given by the indicator map y in Eq. (3). The averaged data have been taken with batch sizes of 100, 1000, and 10 000 in each case. The variance of the Poisson source is seen to diminish around the mean value of 0.5 more rapidly than the intermittent source as the batch size increases.

congestion, i.e., the phase transition or critical point. The *critical point* for a network can be defined as the load for which throughput reaches a maximum. In Fig. 2(b), for example, a plot of throughput against load for a network grid of 32×32 nodes with 164 hosts reaches a maximum at a critical load, $\lambda_c=0.39$. However, it is important to note in Fig. 2(a) (see also Sec. IV) that congestion impacts at a load value lower than the critical load λ_c.

A. Distance model for global critical load

A global approach for estimating λ_c is to consider the total distance all the packets at time t have to travel to reach their destination. At the boundary of the congested phase, there are queues at all nodes, and the change in the total distance is

$$D(N_{t+1})-D(N_t), \tag{5}$$

where N_t is the number of packets in the queues at time t and $D(N_t)$ is the aggregate distance of all these packets from their destinations at time t. At each time step, the number of packets increases by $\rho\lambda L^2$ and their average distance to destination is $L/2$. Thus the overall added distance is $\rho\lambda L^2(L/2)$. By contrast, the aggregate distance is reduced by L^2, given that every packet at the head of the queue moves

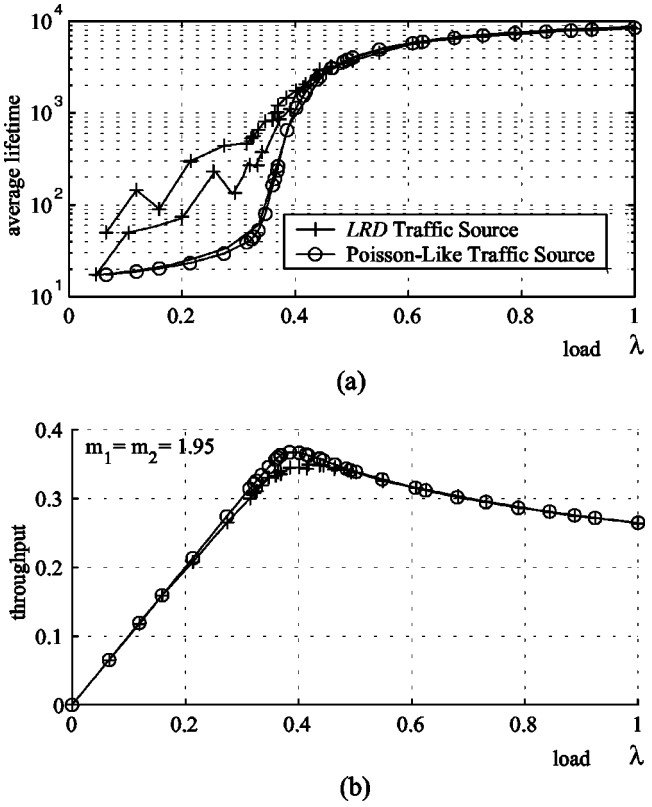

FIG. 2. (a) Average packet lifetimes are plotted as a function of the load λ for Poisson sources and also for LRD sources with increasing average lifetime (in the precongestion phase) as m increases through $m=1.5$,1.8, and 1.95. (b) Corresponding throughputs for Poisson and LRD traffic are plotted as a function of the load λ for $m=1.95$. Note that the lower peak value in throughput for the LRD traffic sources reflects the longer average lifetimes below the critical point. The peak differences diminish to zero as m is decreased to the (Poisson-like) value $m=1.5$.

one step closer to its destination. Thus the change in total distance to destination between time t and $t+1$ is

$$D(N_{t+1})-D(N_t)=\rho\lambda L^2\left(\frac{L}{2}\right)-L^2. \tag{6}$$

The critical load λ_c occurs when the total distance no longer decreases, giving

$$\lambda_c=\frac{2}{\rho L}, \tag{7}$$

(cf. Fig. 3), which corroborates the estimate from the mean field model of Fǔks and Lawniczak [7], who considered the special case $\rho=1$.

B. Average utilization model

The distance model determines the global critical load by assuming that the whole network is fully loaded at each time step, i.e., the aggregate distance reduces by L^2—one packet per node moves one step closer to its destination. This model can be developed further to estimate local critical load conditions by taking into account the different behavior for hosts and routers. Given that hosts also route packets, if o_r is the average utilization of any node queue due only to cross traffic, then the total node utilization across the whole network can be given by

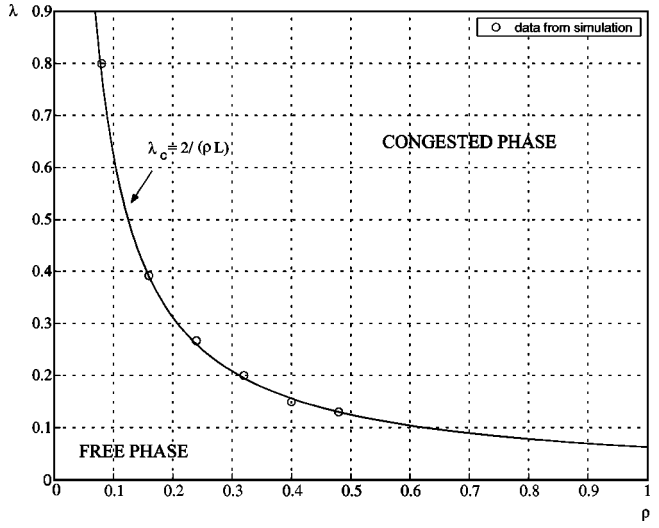

FIG. 3. The mean field boundary, $\lambda_c=2/(\rho L)$, in the (ρ,λ) plane which separates the *free* and *congested* phases. Experimental data for the boundary are also plotted.

$$N=(o_r+\lambda)n_h+o_r n_r, \tag{8}$$

where n_h is the number of hosts and n_r is the number of routers. The local critical load condition is given by

$$o_r+\lambda=1, \tag{9}$$

which implies that the hosts are fully loaded, but that routers are not. So, at each time step the aggregate distance reduces by $N<L^2$.

As before, the overall added distance per time step is $\rho\lambda L^2(L/2)$. Thus the change in total distance to destination between time t and $t+1$ is

$$D(N_{t+1})-D(N_t)=\rho\lambda L^2\left(\frac{L}{2}\right)-[(o_r+\lambda)n_h+o_r n_r]. \tag{10}$$

When the total distance no longer decreases, we obtain the following equation for o_r:

$$o_r=\rho\lambda\left(\frac{L}{2}-1\right). \tag{11}$$

If the average utilization of queues exceeds the rate at which packets are served, then queues will become overloaded. Since routers handle cross traffic exclusively, the average occupancy of router queues is given simply by o_r. For host queues the packets produced by the source have to be added, so the average occupancy is $o_r+\lambda$. For this network packets are always served at the rate of one per time tick, hence if either value exceeds 1 then queues will become overloaded. Substituting the condition for host queues becoming over-

loaded, $o_r+\lambda=1$, into Eq. (11) gives the following expression for λ_c', the load at which (local) congestion starts:

$$\lambda_c'=\frac{1}{\rho\left(\frac{L}{2}\right)-\rho+1}. \tag{12}$$

Congestion is present for loads between λ_c' and λ_c. In this case, host queues are overloaded $o_r+\lambda>1$, and hence increasing in size, and congestion spreads to router queues. However, the router queues are not fully utilized until the global criterion is met at λ_c, when the total service capacity of the network is fully matched by the overall added distance of incoming traffic.

IV. NUMERICAL ANALYSIS OF THE CRITICAL POINT

All our simulations were run first with LRD sources and then with Poisson-like traffic sources for comparison. The LRD data for Fig. 2 are shown for various values of $m_1=m_2$. We have chosen equal intermittency parameters to simplify the interpretation of the observed behavior. In general, the heaviest power-law autocorrelation decay dominates the behavior [13–15]. Values of m_1 and m_2 close to the maximum values of $m_1=m_2=2$ give the highest degree of intermittency and hence the greatest contrast with Poisson traffic sources (corresponding to $m_1=m_2=1.5$ in the intermittency model). The highest value used in our simulation, $H=0.975$, has been observed in statistical investigations [16] of real network traffic data and has been used for most of the data in this paper.

Figure 2 gives a comparison of onset of congestion in two otherwise identical networks with host density $\rho=0.164$, one Poisson sourced, and the other LRD sourced for different values of the Hurst parameter. The values of the intermittency parameters $m_1=m_2=m$ are kept equal in each case for simplicity. Figure 2(a) shows the average lifetime, or *end-to-end delay*, of a packet plotted against load λ, the average number of packets generated per host per unit time. As has been seen in the other models, there is a phase transition from a free phase in which lifetimes remain small to a congested phase in which lifetimes increase rapidly. We first consider the Poisson sources (see Sec. III A). Congestion begins at a load λ_c' that is lower than the critical load λ_c. For this network, Eq. (12) gives a value for λ_c' of 0.30. Below this load, average lifetimes are below 40. This is higher than the approximation of $L/2$ [see Eq. (11)] used in Sec. III A, but of the same order. Beyond this point lifetimes rise exponentially due to congestion. The critical load [as defined by Eq. (7)] for this network is $\lambda=0.39$. Comparing the effect of the different types of traffic source, there is very good agreement above the critical point, in the congested phase. The most pronounced differences do occur near and immediately below the critical point. Below the critical point the average lifetimes for LRD sources are much greater than for Poisson sources—typically ten times as long.

Figure 2(b) shows the throughput versus load. The peak in throughput occurs at the critical point. The network therefore reaches its peak efficiency at the critical point. The peak value of throughput is slightly lower for the LRD sources, emphasizing the longer lifetimes of packets. However, the difference is less pronounced than that seen in average lifetimes. Away from the peak, values of throughput for the two types of traffic source are very similar. Note that when $m_1=m_2=1.5$ the intermittency source behaves like a Poisson source (cf. Ref. [10]).

Figure 2 also shows the effect of decreasing the values of m_1 and m_2 from the maximum 2. The differences between the LRD sources and the Poisson-like sources diminish as expected until the value of $m_1=m_2=1.5$ is reached and the plots become identical. At this point the Hurst parameter is 0.5, equivalent to there being no LRD, the autocorrelation decays exponentially, and so the two sources, i.e., LRD and Poisson, would be expected to be statistically indistinguishable in terms of autocorrelation. One can obtain plots similar to those in Fig. 2, for the range of values of the host density ρ. As ρ increases, the total load on the system increases and the phase transition becomes sharper. This is also seen in other critical phenomena. As predicted by Eq. (7), λ_c decreases as ρ increases. This scaling $\lambda_c\sim\rho^{-1}$ also occurs in Ref. [17]. Plotting λ_c against ρ (Fig. 3) shows good agreement with the theoretical prediction of Eq. (7). Fŭks and Lawniczak [7] also obtained λ_c from their data for the case $\rho=1$.

In Fig. 4, time series of the average host and router queue sizes for a lattice are plotted with the same parameters as for Fig. 2. Figure 4 has a range of load values up to the critical load $\lambda_c=0.39$. These plots confirm that at this point the system has already left the steady state (where there is no upward trend in the number of packets in the system). In the case of Poisson sources. [Fig. 4(a)] the average host queue size starts rising at a load of $\lambda_c'=0.30$, as predicted by Eq. (8), indicating the onset of congestion. Below a load of $\lambda=0.28$, average host queue sizes are approximately equal to average router queue sizes. This indicates the free flowing phase in which packets are fairly evenly spread throughout the network. The greater fluctuations in host queue size are caused by averaging over a smaller number of nodes. At loads above $\lambda_c'=0.30$ both averages rise approximately linearly, with host queue sizes rising at a much greater rate than router queue sizes [cf. Figs. 4(a) and 4(b)].

The equivalent plots for LRD traffic sources in Figs. 4(c) and 4(d) show that the loss of steady state occurs at a much lower value of the load. This corresponds with the earlier rise in average latency displayed in Fig. 2. The average router queue time series are similar to those in Fig. 4(b) for Poisson sources, except for the greater fluctuations. Hence the much higher average lifetimes prior to congestion seen in Fig. 2 are entirely due to delays in host queues. For loads above $\lambda=0.15$, the rate of increase in average host queue size rises rapidly by contrast with the Poisson case.

In actual packet networks, the distance traveled by packets is an important factor. We have investigated the average lifetime and rate of packets delivered as a function of load for a range of path lengths. The transition to congestion can be seen in such plots [18]. Average lifetimes are higher for longer path lengths, as would be expected. For path lengths of 12 steps or more, the throughput reaches a peak and then

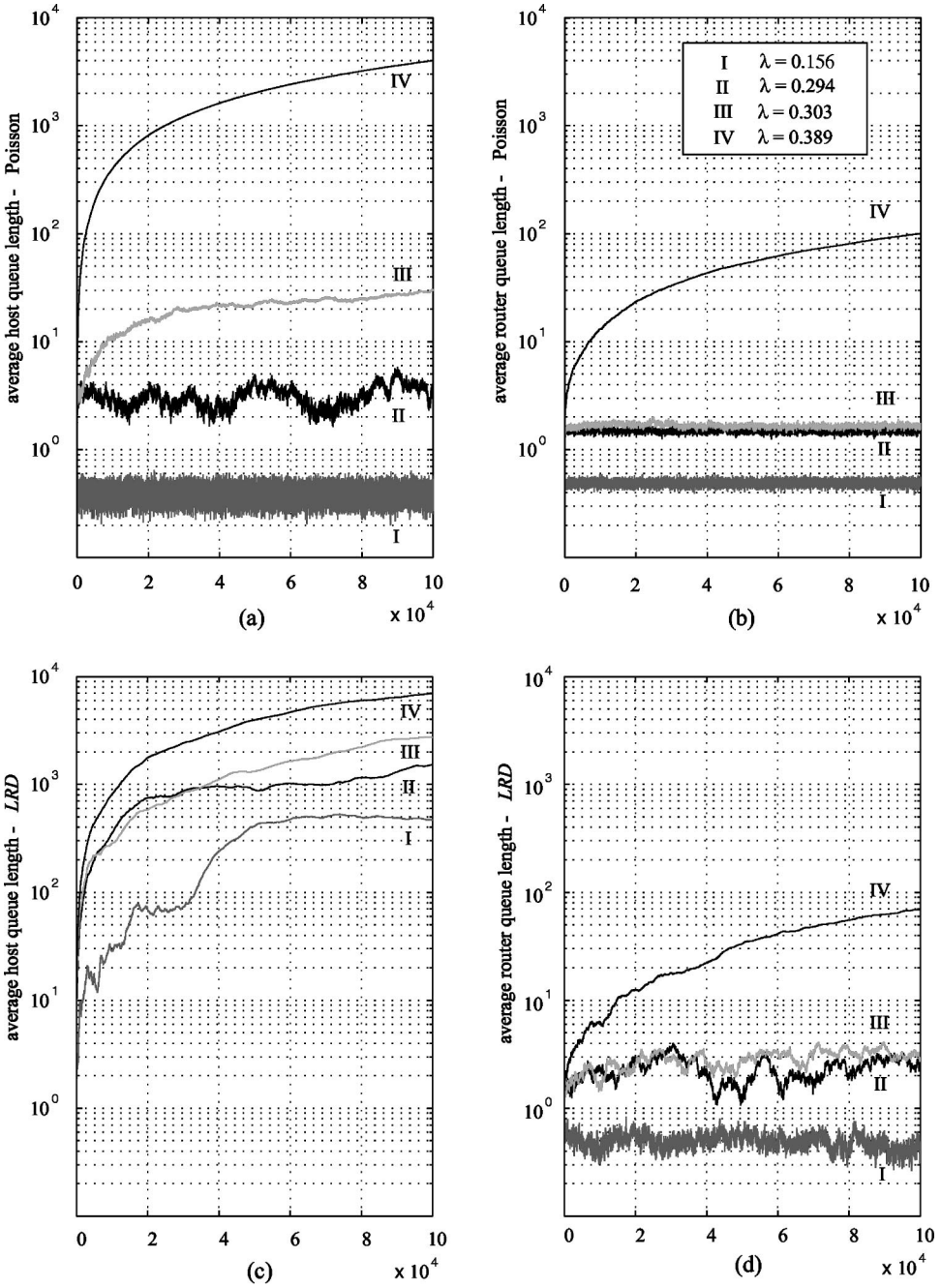

FIG. 4. Time series over 100 000 time units: (a) average host queue length (Poisson); (b) average router queue length (Poisson); (c) average host queue length (LRD); (d) average router queue length (LRD). In each of the parts (a)–(d) plots are given for the four load values $\lambda = 0.156$, 0.294, 0.303, and 0.389 up to the critical network load of $\lambda = 0.39$.

drops off as the load is increased. This is similar to the behavior seen for the average of all path lengths, cf. Fig. 2 and Ref. [18]. For the shorter path lengths the throughput rises slightly with increasing load. This is possibly because the large host queues can be avoided for the majority of short paths, and the rise in router queue lengths has less influence than the rise in the rate of packet creation. Comparing LRD traffic sources with Poisson sources, the features seen in previous plots are present for all path lengths, with decreased throughput near the critical point, and an earlier rise in average latency. Similar plots can be obtained for selected source-destination pairs [18]. A smoothing of the plots away from the critical load arises from averaging data over the various path lengths away from the critical region. The behavior in the critical region is more volatile and the averaging does not provide convergence here. The number of such paths for each path length depends on the lattice size, density of hosts, and selected host pattern. The variation in number of paths and change in lifetime with path length account for the changes in peak value of throughput.

V. TIME SERIES ANALYSIS OF LONG-RANGE DEPENDENCE

Long-range dependence, manifested as power-law decay of the autocorrelation in the time series of queue lengths, has been reported in Refs. [4] and [8]. Since only Poisson traffic sources were used, this autocorrelation behavior must come

TABLE I. The power-law behavior of R/S with respect to the exponent H for path lengths $l=1$ and $l=24$ for hosts with Poisson and LRD characteristics.

	H (Poisson)		H (LRD)	
Load (λ)	$l=1$	$l=24$	$l=1$	$l=24$
0.2	0.51	0.57	0.61	0.61
0.29	0.71	0.70	0.60	0.56
0.30	0.54	0.53	0.61	0.57
0.39	0.52	0.51	0.60	0.54
0.45	0.56	0.55	0.57	0.52

purely from interaction within the network. We investigated this and the effect of replacing the Poisson sources with LRD sources. To expand upon the previous work, we analyzed time series for delays of 1 step and 24 steps, and also looked at time series of average host and router queue lengths measured at each time tick.

Hurst's empirical law for estimating long memory was introduced in 1951 [19], see also Refs. [3,5]. It is obtained by considering the so-called *rescaled data*. More precisely, let X_t, $t\in\mathbb{Z}^+$ denote a discrete time series. The *adjusted range* is defined as

$$R(t,k)=\max_{0\leqslant i\leqslant k} R_i(t,k)-\min_{0\leqslant i\leqslant k} R_i(t,k), \tag{13}$$

where

$$R_i(t,k)=\sum_{l=1}^{t+i} X_l-\sum_{l=1}^{t} X_l-\frac{i}{k}\left(\sum_{l=t+1}^{t+k} X_l-\sum_{l=1}^{t} X_l\right). \tag{14}$$

The quantity $R(t,k)$ is normalized by the translated sample standard deviation

$$S(t,k)=\sqrt{k^{-1}\sum_{l=t+1}^{t+k}(X_l-\overline{X}_{t,k})^2}, \tag{15}$$

where $\overline{X}_{t,k}=k^{-1}\Sigma_{l=t+1}^{t+k}X_l$. The R/S statistic is then defined to be

$$R/S_t(k)=\frac{R(t,k)}{S(t,k)} \tag{16}$$

and it is fitted to the equation

$$\ln E[R/S(k)]=a+H\ln k, \tag{17}$$

with H interpreted as the Hurst parameter.

In Table I we consider separate R/S plots for 1 and 24 step journeys in a 32×32 network grid with 164 hosts for Poisson, and for LRD sources for a range of load values. The network used had the same parameters as that used for Fig. 4, so the onset of congestion at a load of $\lambda=0.3$ was expected. At the smaller loads the network remains free of congestion. This means that time series of packet delays are stationary, and the original data may be used in measuring a value of H. For the higher values of the load, including $\lambda=0.3$, congestion does occur, leading to an upward trend in delay times and queue sizes. In this case, the data are weighted to remove the trend, creating a stationary series. In Table I (Poisson) we see that for $\lambda=0.2$, $H\approx0.5$ for both path lengths, indicating that very little LRD is present. This is corroborated by the probability distributions of delays which both have the characteristic shape of exponentially decaying delay times (see Ref. [18]). However, for $\lambda=0.29$, H values are higher for both path lengths. The R/S plots show a kink with the steeper part of the curve corresponding to $H=0.8$ in both cases. Hence the longer delays (and lower frequencies) do show significant LRD, but this is not seen at any other load value. Values for the three higher load values show very similar H values. Note that in these cases, the time series was weighted to remove the upward trend and the H values are all close to 0.5. This lack of any LRD seems to be caused by the phase change to the congested region above λ_c'. The probability distributions for these higher values show delays shifting towards the length of the run (1×10^6 time ticks) as the network becomes more and more congested. Here 1 and 24 step delays have a long tailed distribution, but this is caused by the nonstationarity of the data, not power-law autocorrelation decay.

TABLE II. R/S behavior for time series of (a) average host; (b) average router queue lengths.

	H (Poisson)		H (LRD)	
Load(λ)	Hosts	Routers	Hosts	Routers
0.2	0.69	0.69	1.0	0.95
0.29	0.96	0.78	1.0	1.0
0.3	0.98	0.89	1.0	1.0
0.39	0.99	1.0	0.99	1.0
0.45	0.98	1.0	1.0	1.0

The LRD data in Table I show values of 0.6 for the 1 step and 24 step data. This is slightly higher than the equivalent data for Poisson sources, but much less than the value for the LRD sources by themselves, i.e., $H=0.975$. If delay probability distributions are compared with the Poisson case then the presence of congestion is indicated by the much longer delay times when LRD sources are used. Similar values of H are seen at higher load values. This suggests that any LRD in the system is not strongly transferred to packet delay times. As before, the distribution of packet delays shifts towards the length of the run as the load increases. This gives a long tailed distribution, but with low H value.

In Table II, high values of H for queue length distributions at hosts and routers are measured at all postcritical loads for Poisson sources indicating the presence of strong network-induced LRD. The R/S values in Table II are calculated from the average host and router queue lengths for the runs used for Table I. For LRD sources, the values of H are all about 1, both for routers and hosts. This shows that the intermittency of the sources has fed through to average queue sizes, both for hosts and routers. For Poisson host queues, H is very high (almost 1) for all load values, except for a load of 0.2, where $H=0.7$. The lower H value at a load of 0.2 agrees to some

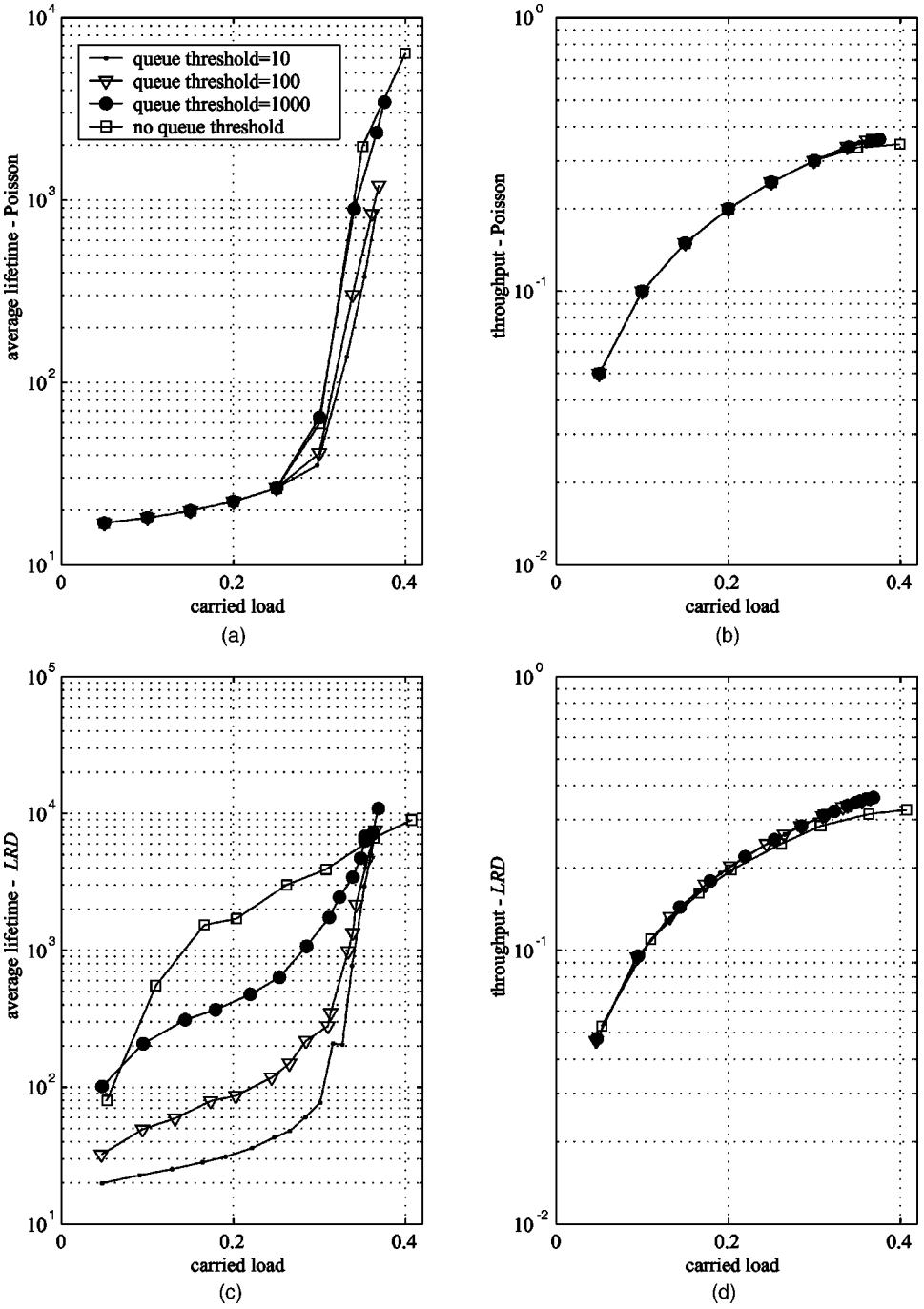

FIG. 5. Plots showing the behavior of the network parameters *average lifetime* and *throughput* as carried load is varied when control is applied to a network containing either all Poisson or all LRD sources. The network modeled is the same as before—32 $\times$32 nodes with 164 hosts. The control mechanism has little effect until the network becomes congested.

extent with the delay distributions for that load, which show an exponential decay. Average Poisson router queue lengths in Table II have slightly lower values of H. This shows that router queues suffer less LRD than host queues. The data for the LRD sources in Table II show that congestion starts at much lower values of the load. For this reason it was necessary to remove trends from all the LRD data used in R/S plots used in Table II.

VI. NETWORK PACKET TRAFFIC SIMULATION WITH CONTROL

The simplest way to control packet traffic is to limit the length of queues [20–22]. As grid bar charts of node queue sizes have shown [18], long queues in the network invariably occur at hosts. For this reason it was decided to reduce the rate of packet production at hosts with long queues. The simulation keeps count of packets produced, so the actual or ''carried'' load is known. Knowledge of the d value being used for the map f gives the maximum rate of packet production, or ''offered'' load.

Figures 5(a) and 5(b) show average lifetime and throughputs plotted against the carried load. The data apply to a 32 $\times$32 node rectangular network with a host density $\rho=0.16$ and Poisson-like traffic sources. A comparison is made between simulations with and without a queue limit. There is little difference between the two cases below a carried load of $\lambda=0.3$. Average lifetime and throughput are very similar.

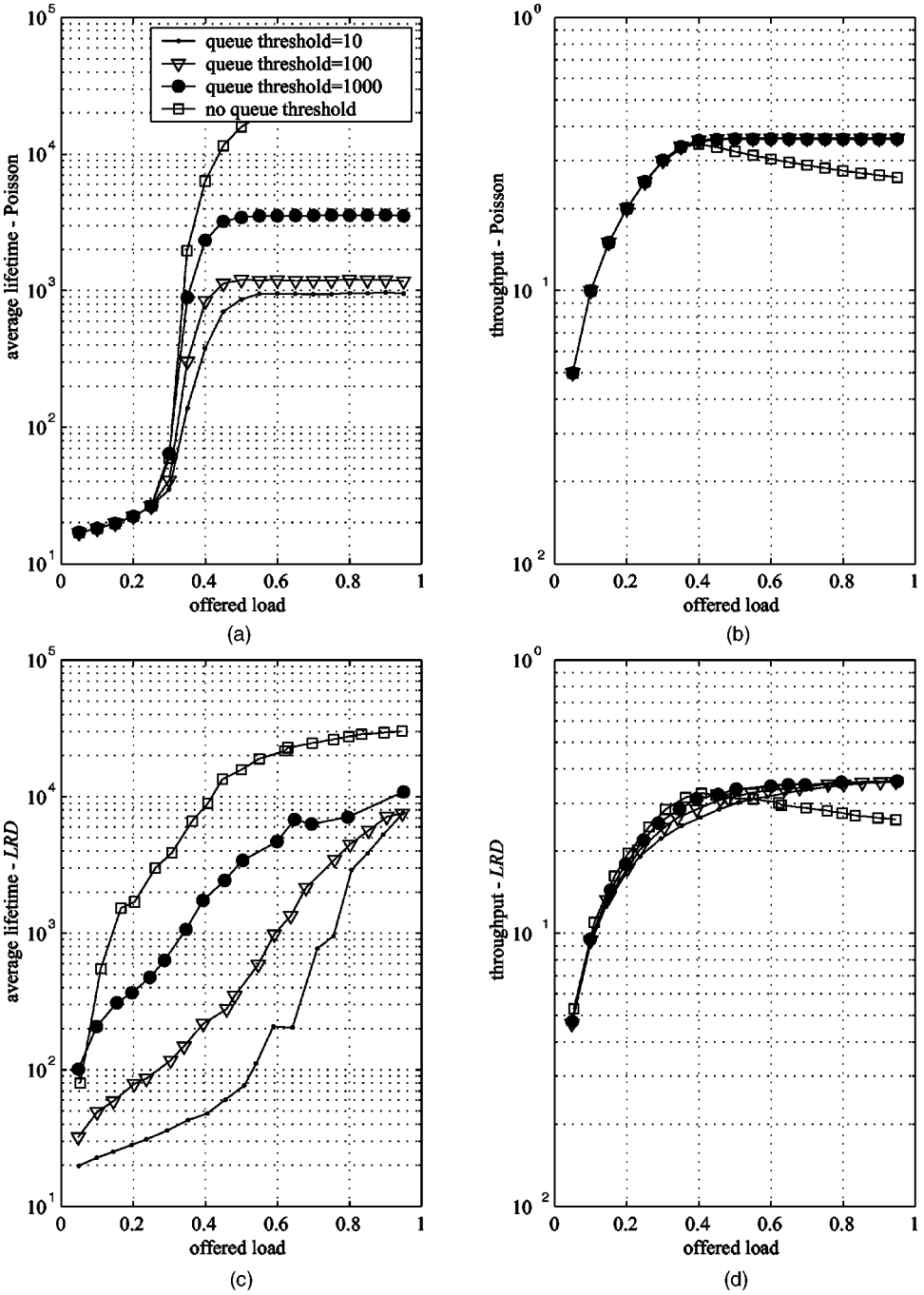

FIG. 6. Plots are as in Fig. 5, but with offered load replacing carried load.

Average queue lengths are closely linked to average lifetime. As has been shown previously, this is the point at which congestion sets in. Above this point average lifetimes and host queue lengths are much lower in the controlled case. In the case of host queue length this would be expected, because when packets are created at a host they are immediately added to the queue for that host. The queue limit device prevents longer queues from building up. This also explains the longer average lifetimes. Long host queues no longer exist, so host packets are not delayed so long and average latency times are therefore lower. The average router queue length is longer in the controlled case because there is no limit on router queue lengths, so that packets that would have been in host queues become distributed over router queues instead. The effect on throughput is much smaller, but there is a slight increase when control is used. It should be noted that the plots do not extend beyond a carried load of about $\lambda = 0.36$, which is the maximum load with queue limiting. In a real network this would equate to bandwidth being traded for reduced end-to-end delay.

Figures 5(c) and 5(d) show similar plots for the same network with LRD sources. In this case the average lifetime is very much lower in the controlled case for the whole range of carried load values. As before, the average queue lengths are linked closely to average lifetime. We have seen in Sec. IV that, in the case of LRD sources, congestion starts at very low values of load. The queue limiting prevents this early onset of congestion, modifying the system to behave as the

same network with Poisson sources would. This can be seen in the plots of average lifetime. Again, higher queue thresholds have less influence. The throughput is slightly higher in the controlled case at high values of the load. As before, the highest possible load when control is used is about $\lambda = 0.36$.

Figures 6(a) and 6(b) show plots of the same parameters for the same network with Poisson sources, but plotted against *offered load* instead of carried load. The plot of average lifetime versus offered load shows that in the controlled case average lifetimes remain low even when they would become very high in the uncontrolled case. The same applies to average host queue sizes. In effect, the control mechanism prevents the network from becoming congested, no matter how high the offered load, but at the expense of restricting the carried load to one that the network can manage. Similar conclusions can be drawn for LRD sources in Fig. 6(c) and 6(d).

VII. SUMMARY AND REMARKS

We have shown that the greatest difference in the behavior of same load Poisson and LRD traffic sources in a model of network traffic occurs close to the critical point. We show that LRD destroys the clean phase transitions apparent for Poisson traffic [17,2,4] and makes the problem of detecting onset of congestion much more problematical. Most importantly, below criticality, average packet lifetimes for LRD sources are much higher, and at criticality, the packet throughput is decreased.

There are essentially three load types for Poisson-like sources: (i) at low loads, packets travel freely through the system—little LRD is present, average lifetimes are close to the source to destination distance as queues are small; (ii) at a well-defined load, $\lambda = \lambda_c' < \lambda_c$, local congestion sets in, host queues become overloaded, and the system is no longer in a steady state, but most offered load still reaches its destination in this precongestion phase and LRD throughput is decreased at criticality; (iii) beyond the critical point, router queues are overloaded and the network is increasingly congested. It should be noted that a significant degree of self-similarity can be seen in packet delay times in the precongestion phase which disappears when congestion starts.

Congestion begins at a much lower load value for LRD sources, but the critical point, at which throughput reaches a maximum, is similar to the Poisson critical load value. The mechanism causing the earlier onset of congestion is not fully understood, see Takayasu *et al.* [23], but is probably associated with phase transitions in thermodynamic functions (see Refs. [24,11]). But other factors such as the spatial distribution of congested nodes [25], are important. More sophisticated routing algorithms than those considered here can address this problem. Also, R/S behavior in Tables I and II, and probability distributions of packet delays [26,18] showed that when networks are congested little LRD is seen in delay distributions. These show that long tails are present when congestion occurs, but this appears to be caused by the nonstationarity of the data, rather than any LRD.

Mean field approaches give a value for the critical load λ_c at which throughput reaches a maximum, and predicts the point at which local congestion starts quite accurately. Theoretically the sharpness of this phase transition should increase with increasing total load on the network. This is seen in the data, since increasing the host density does sharpen the transition [18]. We also see that the maximum efficiency of the system, in terms of throughput, occurs at the critical point. This agrees with other data network models, notably Ref. [4], and is also seen in models of road traffic [27].

Application of a simple control mechanism showed that the network can be prevented from becoming congested by effectively limiting its packet carrying capacity. Extra refinements in routing and network information carried by the packet are being considered; see also Refs. [17,28,29,23] for current progress. The key aim is to develop the uncontrolled model into one which reacts to the local buildup of queues [20], with an objective of delaying the onset of congestion at the network level when the sources are strongly long-range dependent.

[1] W. E. Leland, M. S. Taqqu, W. Willinger, and D. V. Wilson, Comput. Commun. Rev. **23**, 183 (1993).

[2] M. Takayasu, H. Takayasu, and T. Sato, Physica A **233**, 824 (1996).

[3] J. Beran, *Statistics of Long Memory Processes*, Monographs on Statistics and Applied Probability Vol. 61 (Chapman and Hall, London, 1994).

[4] R.V. Solé and S. Valverde, Physica A **289**, 595 (2001).

[5] J. Feder, *Fractals* (Plenum, New York, 1988).

[6] T. Ohira and R. Sawatari, Phys. Rev. E **58**, 193 (1998).

[7] H. Fŭks and A.T. Lawniczak, Math. Comput. Simul. **51**, 101 (1999).

[8] J. Yuan, K. Mills, and D. Montgomery, w3.antd.nist.gov/~mills/unpublis.htm

[9] A. Erramilli, R.P. Singh, and P. Pruthi, in *Proceedings of the 14th International Teletraffic Conference 1994*, edited by James W. Roberts (North-Holland, Elsevier, Amsterdam, 1994), pp. 329–38.

[10] H.G. Schuster, *Deterministic Chaos: An Introduction*, 3rd (VCH, Weinheim, 1995), pp. 91–97.

[11] X.-J. Wang, Phys. Rev. A **40**, 6647 (1989).

[12] A. Lasota and M.C. Mackey, *Chaos, Fractals and Noise* (Springer, New York, 1994).

[13] M.S. Barenco and D.K. Arrowsmith (unpublished).

[14] A. Giovanardi, G. Mazzini, and R. Rovatti, in *Proceedings of NOLTA 2000*, edited by Shin'ichi Oishi and Wolfgang Schwarz (w.e.b. Universitätsverlag and Buchhandel, Dresden, 2000), pp. 747–750.

[15] R.J. Mondragón, Int. J. Bifurcation Chaos Appl. Sci. Eng. **9**, 1381 (1999), see Ref. [11].

[16] B. Bogacka and M. Keogh-Brown, (private communication).

[17] S. Valverde and R.V. Solé, Physica A **312**, 636 (2002).

[18] M. Woolf, D.K. Arrowsmith, R.J. Mondragón, and J.M. Pitts, www.maths.qmul.ac.uk/~arrow/netfigs.pdf.
[19] H.E. Hurst, Trans. Am. Soc. Civ. Eng. **116**, 770 (1951).
[20] I. Csabai, J. Phys. A **27**, L417 (1994).
[21] R.J. Mondragón, D.K. Arrowsmith, and J.M. Pitts (unpublished).
[22] R.J. Mondragón, J.M. Pitts, and D.K. Arrowsmith, in *Proceedings of the XVIII World Telecommunications Congress*, Paris, 2000, edited by A. Vomscheid and P, Chemouil (SEE, Paris, 2000), Vol. 12(4), p. 1.
[23] K. Fukuda, H. Takayasu, and M. Takayasu, Physica A **287**, 289 (2000).
[24] R. Albert and A.-L. Barábasi, e-print cond-mat/0106096.
[25] P. Bak and K. Chen, Phys. Lett. A **147**, 297 (1990).
[26] J.M. Pitts, J.A. Schormans, M. Woolf, R.J. Mondragón, and D.K. Arrowsmith, IEEE Trans. Acoust., Speech, Signal Process **4**, 4044 (2002).
[27] K. Nagel and M. Schreckenberg, J. Phys. I **2**, 2221 (1992).
[28] M. Takayasu, K. Fukuda, and H. Takayasu, Physica A **274**, 140 (1999).
[29] M. Takayasu, K. Fukuda, and H. Takayasu, Physica A **277**, 248 (2000).